Improved thermostability of Bacillus circulans cyclodextrin glycosyltransferase by the introduction of a salt bridge

Leemhuis, H; Rozeboom, HJ; Dijkstra, BW; Dijkhuizen, L; Dijkstra, Bauke W.

Published in:
Proteins-Structure Function and Bioinformatics

DOI:
10.1002/prot.10516

Publication date:
2004

Improved Thermostability of *Bacillus circulans* Cyclodextrin Glycosyltransferase by the Introduction of a Salt Bridge

Hans Leemhuis,[1] Henriëtte J. Rozeboom,[2] Bauke W. Dijkstra,[2] and Lubbert Dijkhuizen[1]*

[1]*Department of Microbiology, Groningen Biomolecular Sciences and Biotechnology Institute (GBB), University of Groningen, Kerklaan 30, 9751 NN Haren, The Netherlands*

[2]*BIOSON Research Institute and Laboratory of Biophysical Chemistry, GBB, University of Groningen, Nijenborgh 4, 9747 AG Groningen, The Netherlands*

ABSTRACT **Cyclodextrin glycosyltransferase (CGTase) catalyzes the formation of cyclodextrins from starch. Among the CGTases with known three-dimensional structure, *Thermoanaerobacterium thermosulfurigenes* CGTase has the highest thermostability. By replacing amino acid residues in the B-domain of *Bacillus circulans* CGTase with those from *T. thermosulfurigenes* CGTase, we identified a *B. circulans* CGTase mutant (with N188D and K192R mutations), with a strongly increased activity half-life at 60°C. Asp188 and Arg192 form a salt bridge in *T. thermosulfurigenes* CGTase. Structural analysis of the *B. circulans* CGTase mutant revealed that this salt bridge is also formed in the mutant. Thus, the activity half-life of this enzyme can be enhanced by rational protein engineering. Proteins 2004;54:128–134.**

Key words: alpha-amylase family; CGTase; mutagenesis; starch; structure

INTRODUCTION

CGTase is a member of glycoside hydrolase family 13,[1] the α-amylase family.[2,3] All members of this family use an α-retaining mechanism[4,5] to catalyze a variety of reactions, including hydrolysis and transglycosylation of α-(1,4)- and α-(1,6)-glycosidic bonds.[6,7] CGTase produces cyclodextrins from starch, which are circular molecules composed of 6, 7, or 8 glucose residues linked via α-(1,4)-glycosidic bonds (α-, β- and γ-cyclodextrin, respectively). The reaction proceeds via a covalent glycosyl–enzyme intermediate.[5,8] In the cyclization reaction, the nonreducing end of this intermediate moves into acceptor subsite +1, which is followed by intramolecular bond formation. CGTase may also transfer the covalently bound intermediate to water (hydrolysis reaction), or to the nonreducing end of a second sugar, to yield a linear product (disproportionation reaction). Interestingly, the hydrolytic activity of CGTase is much lower than its transglycosylation activities, making the enzyme an efficient transferase.[9]

Three-dimensional (3D) structures of 5 CGTases are known from *Bacillus circulans* strains 8[10] and 251 (BC251),[11] *Thermoanaerobacterium thermosulfurigenes* strain EM1 (*Tabium*),[12] *Bacillus stearothermophilus*,[13] and alkalophilic *Bacillus* sp. 1011.[14] The structures are organized in 5 domains (A–E). The N-terminal part consists of a catalytic $(\beta/\alpha)_8$-barrel fold (domain A), with a loop of approximately 60 residues protruding at the third β-strand (domain B). Domains A and B together form the substrate binding cleft.[15] Domain E is a starch-binding domain,[16,17] whereas the functions of domains C and D are not known.

Despite this detailed structural knowledge, the structural basis for thermostability of CGTases is far from being understood.[18] Among the CGTases with known 3D structures, *T. thermosulfurigenes* CGTase has the highest thermostability,[12,19–21] (with an activity half-life of 15 min at 90°C[19]). Other CGTases with known 3D structures have activity half-lives of 10 min at 60°C (BC251 CGTase) and 10 min at 75°C (*B. stearothermophilus* CGTase).[20] Yet other CGTases exist with even higher activity half-lives, such as the *Thermococcus kodakaraensis* KOD1[22] and *Thermococcus* strain B1001[23,24] CGTases, with half-lives of 20 min at 100°C and 40 min at 110°C, respectively. Note that these half-lives have not been determined under identical conditions (e.g., different buffers and Ca^{2+} concentrations).

To study the thermostability of CGTases, the available CGTase structures were compared, and selected differences were introduced into BC251 CGTase via site-directed mutagenesis. This yielded a mutant CGTase with a strongly increased activity half-life.

MATERIALS AND METHODS

Structure Determination

Crystals of mutant 9 (T185S, T186Y, N188D, and K192R) were grown from 60% (v/v) 2-methy1-2,4-pentanediol, 100 m*M* *N*-2-hydroxyethylpiperazine-*N*′-2-ethanesulfonic acid (HEPES) pH 7.5, and 5% (w/v) maltose.[11] Data were collected at 100 K on an in-house MARCCD system

Abbreviations: BC251, *Bacillus circulans* strain 251; CGTase, cyclodextrin glycosyltransferase; DSC, differential scanning calorimetry; PCR, polymerase chain reaction; *Tabium, Thermoanaerobacterium thermosulfurigenes* strain EM1.

Grant sponsor: Danisco (H.L.).

*Correspondence to: E-mail: L.Dijkhuizen@biol.rug.nl

Received 17 February 2003; Accepted 09 May 2003

TABLE I. Data Collection Statistics and Quality of the *B. circulans* CGTase Mutant 9

Data collection	
Space group	$P2_12_12_1$
Cell axes *a, b, c* (Å)	117.2, 109.6, 65.7
Resolution range (Å)	32.0 − 2.0
Total no. of observations	363,420
No. of unique reflections	57,077
Completeness (%)[a]	98.8 (96.3)
$\langle I/\sigma(I)\rangle$[a]	34.7 (8.9)
R_{merge} (%)[a]	3.2 (11.5)
Refinement statistics	
Average *B*-factor	18.3
Final *R*-factor (%)[a]	15.2 (18.6)
Final free *R*-factor (%)[a]	17.6 (22.4)
RMSD from ideal geometry	
Bond lengths (Å)	0.005
Angles (°)	1.2
Dihedrals (°)	24.4
Improper dihedrals (°)	0.69

[a]Highest resolution shell in parentheses.

(MarUSA, Inc., Evanston, IL), with a diameter of 165 mm, with the use of CuKα radiation from a BrukerNonius FR591 rotating-anode generator equipped with Osmic mirrors. Processing of the diffraction data was performed with DENZO and SCALEPACK.[25] We used the structure of BC251 CGTase with bound maltotetraose [Protein Data Bank (PDB) code: 1CXF], with all water and sugar molecules removed, as starting model for the refinement [Crystallography & NMR System (CNS)[26]. Ligands were placed in sigmaA-weighted $2F_o$-F_c and F_o-F_c electron density maps with the program O.[27] Data and refinement statistics are given in Table I. The atomic coordinates and the structure factors of mutant 9 have been deposited in the PDB (code 1PYg.pdb; www.rcsb.org).

Bacterial Strains, Plasmids, and Growth Conditions

Escherichia coli MC1061[28] was used for recombinant DNA manipulations. CGTase proteins were produced with the α-amylase and protease negative *B. subtilis* DB104A.[29] Plasmid pDP66k-,[16] containing the *cgt* gene, was used for site-directed mutagenesis and enzyme production. Plasmid-carrying strains were grown on LB[30] medium at 37°C in the presence of kanamycin, 50 or 5 μg/mL for *E. coli* or *B. subtilis*, respectively. Transformation of *B. subtilis* was performed according to the method of Bron.[31]

DNA Manipulations

Mutant CGTases were constructed with PCR, as described.[9] The PCR products were cut with *Pvu*II/*Sal*I or *Sal*I/*Hind*III and exchanged for the corresponding fragment of pDP66k-. The following oligonucleotides were used: 5′-TACAGCATCATCCCTGATTCCACCTTCGGCGGATCCACGGCCTATCAC-3′ (mutant 1); 5′-GAGCGTTTCCACAACGGCGGATCCACCCGGAAGCTGGA-3′ (mutant 2); 5′-TGGCAGTACACCTCGAGCTCGAACTCGCCGACCATC-3′ (mutant 3); 5′-TACTTCGGTACGACGGCGGGAACAATTGTGTCTTGGGAAGACACGCAGAT-3′ (mutant 4); 5′-TTGAAAAAACAAGGCAACACCATCACGTGGGAA-3′ (mutant 5); 5′-TTATCGGTAGCCTCCGACGGATCCGTCACCCCGTTCACGCTTGC-3′ (mutant 6); 5′-GGAACTGGGACACGTCGAAAGCAATCGG-3′ (mutant 7); 5′-TGCACGAACCTCAAACTGTATTGCGGC-3′ (mutant 8); 5′-GACTTTTCCTCGTACGAAGACGGCATCTACCGCAACCTGTACGA-3′ (mutant 9); 5′-AGCTTTATGGATTCCATCAACAACT AT-3′ (mutant 10); 5′-TCCGGCCGTCACGCCCGGGAAATACAACATTA-3′ (mutant 11); 5′-ACGGACTTTTCCTCGACCGAAAACGG-3′ (T185S); 5′-GACTTTTCCACGTACGAAAACGGCATC-3′ (T186Y); 5′-TCCACGACCGAAGACGGCATCTACAA-3′ (N188D); 5′-AACGGCATCTACCGCAACCTGTACGAT-3′ (K192R); 5′-TCCACGACCGAAGACGGCATCTACCGCAACCTGTACG-3′ (N188D/K192R). We constructed mutant 12 using plasmid DNA of mutant 1 as PCR template and the oligonucleotide of mutant 8. All mutations were confirmed by DNA sequencing of the *Pvu*II/*Sal*I or *Sal*I/*Hind*III fragment obtained with PCR.

Enzyme Assays and Enzyme Purification

CGTase proteins were produced and purified as described.[9] The *Tabium* CGTase we used had been purified previously.[32] All enzyme assays were performed in 10 m*M* sodium citrate buffer (pH 6.0) at 50 and 60°C for BC251 and *Tabium* CGTase, respectively. We determined the cyclization activity by incubating 0.2–0.5 μg enzyme/mL with 2.5% (w/v) partially hydrolyzed potato starch (Paselli SA2; AVEBE, Foxhol, The Netherlands). The amount of β-cyclodextrin formed was quantified with phenolphthalein.[33] One unit of activity is defined as 1 μmol of β-cyclodextrin formed per min. The disproportionation activity was determined as described,[34,35] with 0.1–0.5 μg/mL enzyme, 4-nitrophenyl-α-D-maltoheptaoside-4-6-O-ethylidene (Megazyme, County Wicklow, Ireland) as donor substrate, and maltose as acceptor substrate. One unit of activity is defined as 1 μmol of donor substrate cleaved per min. The hydrolyzing activity was determined as described,[9] with 5 μg enzyme/mL and 1% (w/v) soluble starch (Lamers & Pleuger, Wijnegen, Belgium). One unit of activity is defined as 1 μmol of reducing ends formed per min.

CGTase Stability

Resistance to thermal inactivation was determined by incubating 20 μg/mL CGTase in 10 m*M* sodium citrate buffer, pH 6.0, supplemented with 1 m*M* $CaCl_2$ at 60°C. Samples were taken at several time intervals and the residual activity was determined with the disproportionation assay. The activity half-life ($t_{\frac{1}{2}}$) is defined as the time at which half of the initial activity is retained.

Differential Scanning Calorimetry (DSC)

Thermal unfolding was measured with use of the MicroCal VP-DSC microcalorimeter (MicroCal, Inc., Northampton, MA). The cell volume was 0.5 mL, and the experiments were performed with a scan rate of 1°C/min at a constant pressure of 2.75 bar. Samples were degassed

TABLE II. Residues Forming Surface Salt Bridges Typical for *Tabium* CGTase and the Corresponding Residues in BC251 and *B. stearothermophilus* CGTase

Tabium	BC251	*B. stearothermophilus*
Lys 47/Asp89	Arg47/Asn88	Arg44/Asn85
Asp189/Arg193	Asn188/Lys192	***Asp189/Arg193***
Asp245/Lys510	Ala244/Lys510	***Asp245/Lys510***
Glu276/Lys557	Glu275/Asn560	***Glu276/Lys557***

The presence of an interaction between the residues is indicated by bold-italic letters.

prior to the scan. The enzyme concentration we used was 400 μg/mL in 50 m*M* sodium acetate buffer, pH 5.5. The $CaCl_2$ concentration was 10 m*M*.

Structure Comparison

We displayed and compared 3D structures using the Swiss-Pdb Viewer version 3.7 (b2).[36] Superposition of C_α backbone atoms was performed with the standard superposition tools of the program. The following structures were used: *Tabium* CGTase (PDB[37] code: 1CIU[12]), *B. circulans* strain 8 (1CGT[10]) and strain 251 CGTase (1CDG[11]), *B. stearothermophilus* CGTase (1CYG[13]) and *Bacillus* sp. 1011 CGTase (1PAM[14]). Figures were made with the Swiss-PdbViewer, version 3.7b2, and Pov-Ray for Windows, version 3.1 g.

RESULTS AND DISCUSSION

Structural Comparison of CGTases

The overall folds of the 5 CGTases with known 3D structure are very similar, with root-mean-square deviations (RMSDs) below 1 Å.[12] Among these CGTases, *Tabium* CGTase has the highest resistance to thermal inactivation. To study whether any structural differences might cause the difference in thermostability, we compared the structures. Significant differences between BC251 and *Tabium* CGTase (which have 68% amino acid sequence identity and show an overall RMSD of 0.8 Å in their Cα positions) were identified in the loop regions 88–94, 334–339, 494–498, 536–542, and 658–660 (BC251 CGTase numbering). Additional differences between *Tabium* and *B. circulans* strain 8 CGTase were found in loops 472–479 and 618–619.[12] To investigate the contributions of these loop regions to the thermostability, the *Tabium* loops were introduced into BC251 CGTase (mutants 1 to 7).[12] All these loops are located at the surface of the enzyme. However, their importance is not known for either enzymatic activity or thermostability.

Furthermore, surface salt bridges typical for *Tabium* CGTase may also contribute to the relatively high thermostability of this enzyme.[12] *Tabium* CGTase has four salt bridges without counterparts in BC251, *Bacillus* sp. 1011, or *B. circulans* strain 8 CGTase, whereas three of these interactions are found in *B. stearothermophilus* CGTase. The residues forming these salt bridges in *Tabium* CGTase, and the corresponding BC251 and *B. stearothermophilus* CGTase residues, are summarized in Table II. The residues forming the salt bridges in *Tabium* CGTase were also introduced into BC251 CGTase (mutants 9–12) to study the contributions of these interactions on the activity half-lives. Mutant 12 is the combination of mutants 1 and 8.

Enzymatic Properties of Mutant CGTases

All CGTase mutants were successfully constructed, produced, and purified. Only mutant 10 had strongly decreased enzyme activities (Table III). The cause for this is unclear, because the mutations are far from the active-site cleft. The nearly unchanged hydrolytic activities of the mutants (Table III) were somewhat unexpected, because *Tabium* CGTase has a much higher hydrolytic activity than BC251 CGTase (Table III),[19] and the mutations increased the similarity to *Tabium* CGTase (the amino acid sequence identity increased by 1–9 residues in the different mutants). The mutations are, however, remote from acceptor subsites +1 and +2, which is the location where mutations have been shown to have the largest effect on the hydrolytic activity of CGTase.[32,35,38] The relatively small effects on the cyclization and disproportionation activities were, on the other hand, expected, because the mutations we introduced were far from the substrate-binding subsites, except the mutations in the residues Arg47 and Tyr89 at subsite −3[15,39] (mutants 1, 8, and 12). However, mutation studies have shown that Arg47 and Tyr89 are not essential for enzyme activity.[40,41] Thus, the mutants are useful to study the activity half-lives of CGTase.

Activity Half-Lives of (Mutant) CGTases

The activity half-lives of the (mutant) CGTases were determined by incubating the enzymes at 60°C in sodium citrate buffer, pH 6.0, supplemented with 1 m*M* $CaCl_2$. Subsequently, the residual activity was measured as a function of the incubation time. Under these conditions, BC251 CGTase had an activity half-life ($t_{\frac{1}{2}}$) of 9.7 min, whereas *Tabium* CGTase retained full activity after 24 h of incubation (Table III). Most mutations had no large effect on the half-lives, although 3 mutants (1, 10, and 11) had clearly reduced half-lives (Table III). The reason for this is not known. None of the loop differences increased the activity half-life of BC251 CGTase (mutants 1–7). Likewise, of the 4 salt-bridge mutants (mutants 9–12), 3 did not improve the activity half-life of the enzyme. Only mutant 9, designed to provide an extra salt bridge on the surface of the enzyme, showed a significantly increased half-life (7.5-fold; Table III). Thus, most of the loop changes do not (directly) increase the activity half-life of BC251 CGTase. An explanation maybe that some of the mutations have increased the stability of the enzyme locally, but if this part of the enzyme was not limiting the activity half-life of BC251 CGTase, this will not be observed when measuring activity half-lives. In this case, these mutations may contribute to the activity half-life of BC251 CGTase after other stabilizing mutations have been introduced elsewhere in the enzyme (e.g., mutation 9). A second explanation is that some of the differences simply are not responsible for the different activity half-lives of BC251 and *Tabium* CGTase.

TABLE III. Enzyme Activities and Activity Half-Lives ($t_{\frac{1}{2}}$) of the (Mutant) CGTases at 60°C

(Mutant) CGTases	BC251	*Tabium*	Cycl. (U/mg)	Hydr. (U/mg)	Disp. (U/mg)	$t_{\frac{1}{2}}$ (min)
BC251	Wild-type		269	3.2	970	9.7
1	88-NYSGVNN	89-PDSTFGGS	286	3.0	733	4.8
2	334-ASNANR	335-NGGST	234	3.4	629	9.4
3	494-AATAT	494-SSSNSP	253	2.9	924	9.6
4	536-VSGADIT	536-GTIV	248	3.1	941	8.4
5	658-STV	655-NTI	247	3.1	930	8.9
6	472-GSGGAASN	471-ASDGSVTP	274	3.6	1149	8.4
7	618-PA	615-TS	264	3.2	901	8.2
8	47-R	47-K	202	2.3	820	12.2
9	185-TTENGIYK	186-SYEDGIYR	310	3.7	1201	73
10	244-AAV	245-DSI	42	0.4	52	3.9
11	558-GGN	555-PGK	217	4.0	889	3.9
12	Combination of 1 & 8		303	3.0	987	7.0
T185S			284	3.0	946	14.8
T186Y			261	2.8	981	8.0
N188D			302	2.9	1043	35
K192R			251	3.3	841	11.6
N188D/K192R			293	3.1	1012	56
Tabium	Wild-type		240	54	510	$\gg$[a]

Abbreviations: Cycl., cyclization; Hydr., hydrolysis; Disp., disproportionation.
[a]No measurable loss of activity after 1 day of incubation.
In mutants 1–12, the indicated sequence of BC251 CGTase was replaced by sequence shown for *Tabium* CGTase.

To determine whether the enhanced activity half-life at 60°C of mutant 9 was indeed caused by the N188D and K192R mutations, all 4 amino acid differences in mutant 9 (T185S, T186Y, N188D, and K192R) were constructed as single mutants. The double mutant N188D/K192R was made as well. These 5 mutants had similar catalytic activities as wild-type CGTase (Table III). Except for the single N188D mutant and the double N188D/K192R mutant, all had activity half-lives similar to that of wild-type CGTase (Table III). Thus, residues 185 and 186 do not significantly contribute to the activity half-life of CGTase. In contrast, the strongly increased half-lives of the single N188D mutant and the double N188D/K192R mutant suggest that Asp188 can form a stabilizing interaction with either Lys192 or Arg192. The double N188D/K192R mutant showed a half-life increased to 56 min at 60°C, which is slightly shorter than that of mutant 9 (73 min; Table III). Thus, the resistance to thermal inactivation of BC251 CGTase is strongly enhanced by an N188D mutation in the B-domain of the enzyme. Yet the activity half-life of the BC251 CGTase mutants is still far off from the *Tabium* CGTase half-life, indicating that the introduced salt bridge is only one of the stabilizing amino acid substitutions between the two enzymes. Among the other amino acid differences there must be factors that also contribute to the enzyme's activity half-life.

X-Ray Structure of Mutant 9

Mutant 9 was designed to introduce a salt-bridge interaction between Asp188 and Arg192, equivalent to the situation in *Tabium* CGTase (Fig. 1). To ascertain whether this salt bridge had formed, we determined the 3D structure of this mutant. Compared to wild-type CGTase, the protein backbone conformation was not affected by the mutations. The salt bridge between Asp188 and Arg192 is indeed present (Fig. 1), although the Asp188 sidechain interacts with the Nε atom of the arginine sidechain, and not with one of the Nη atoms, as observed in *Tabium* CGTase. The interaction with the Nε atom is identical to the arrangement seen in *B. stearothermophilus* CGTase (Fig. 1).[13] The B-factors of Asp188 (13–17) and Arg192 (13–15) are somewhat below average (18), indicating that these residues are well defined. Besides the Asp188/Arg192 salt bridge, the Arg192 sidechain (Nη atom) also forms an interaction with Asn178 (O atom), that is not present in wild-type BC251 CGTase, but is found in *Tabium* and *B. stearothermophilus* CGTase. The Asn178/Arg192 interaction may also contribute to the activity half-life of the N188D/K192R mutants. Thus, the activity half-life at 60°C of BC251 CGTase is strongly increased by the N188D/K192R mutations, which introduce an extra salt-bridge interaction at the surface of the enzyme.

The enhanced activity half-life at 60°C of mutant 9 reveals that mutations in the B-domain can increase the activity half-life of BC251 CGTase. A strong effect of mutations in the B-domain on activity half-lives has been shown before for other α-amylase family enzymes. In *Pyrococcus furiosus* α-amylase, a Zn^{2+}-binding Cys, located in the B-domain, is essential for the high activity half-life,[42] whereas the activity half-lives of *Bacillus* KSM-1378[43] and *Bacillus licheniformis*[44,45] α-amylase were significantly increased by mutations in their B-domains. Thus, CGTase mutations in the B-domain can also modulate the activity half-life of the enzyme. An explanation for the identification of mutations in the B-domain might be

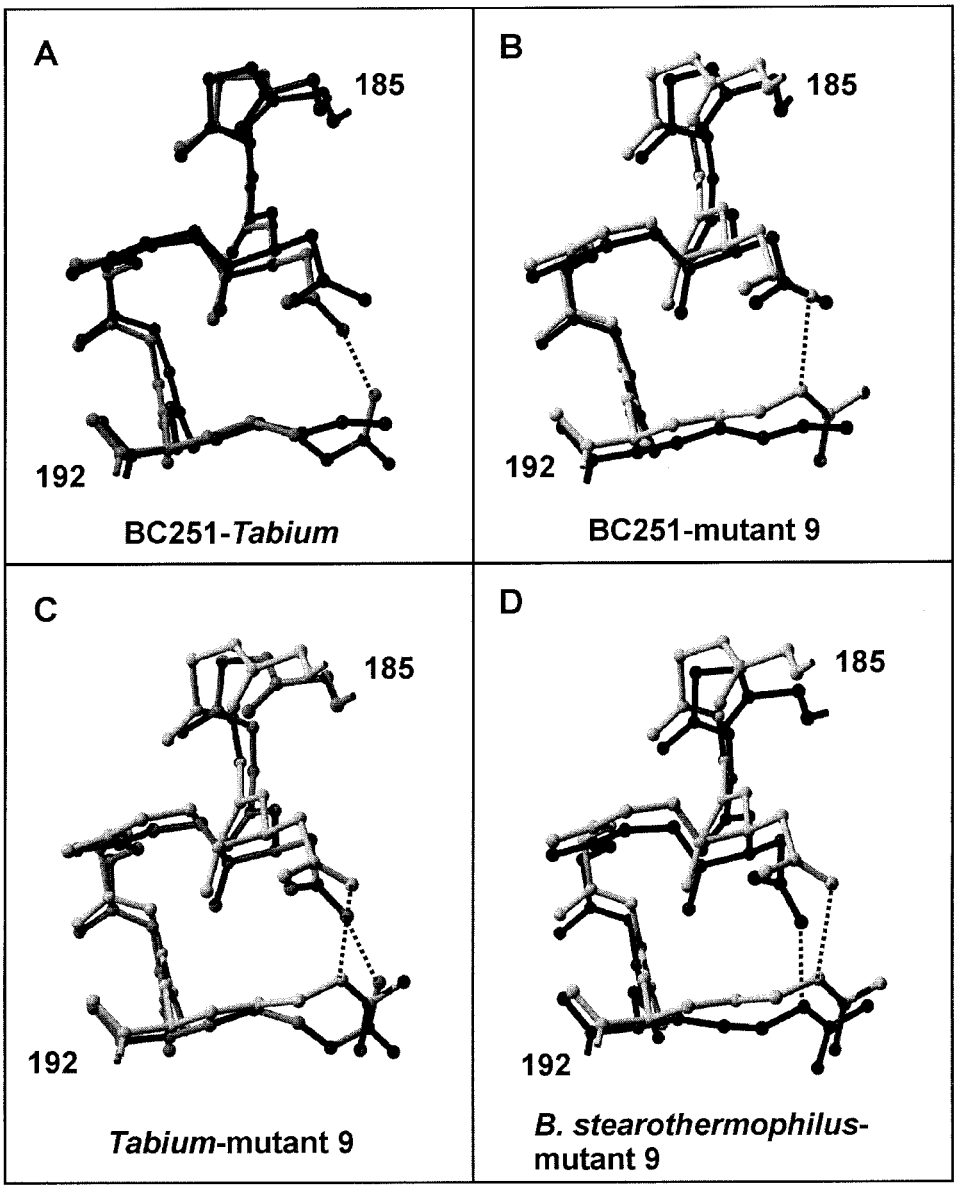

Fig. 1. Close-up views of the loop region 185–192 in CGTase. For clarity, only the backbone and the sidechains of residues 188 and 192 are shown (Asn/Lys in BC251 CGTase; Asp/Arg in *Tabium, B. stearothermophilus*, and mutant 9 CGTases). (**A**) BC251 and *Tabium* CGTase, (**B**) BC251 and mutant 9 CGTase, (**C**) *Tabium* and mutant 9 CGTase, and (**D**) mutant 9 and *B. stearothermophilus* CGTase. Salt bridges are indicated by dashed lines. The CGTases are shown in black (BC251 and *B. stearothermophilus*), gray (*Tabium*), and light gray (mutant 9).

that activity half-lives deal with the active-site environment, and the B-domain is part of this active site.

Differential Scanning Calorimetry

To test whether the increased activity half-life of mutant 9 is accompanied by an enhanced denaturation temperature, we carried out DSC measurements on mutant 9 and wild-type CGTase. Although the unfolding of the CGTases was scan-rate dependent and irreversible (data not shown), this experiment revealed that mutant 9 denatured at a significantly higher temperature than wild-type BC251 CGTase, but still at a much lower temperature than *Tabium* CGTase (Fig. 2). This indicates that the introduced salt bridge is only one of the stabilizing amino acid differences between the two CGTase enzymes. Other mutations are likely to increase the enzyme's denaturation temperature further. However, more investigations are needed to corroborate this. The DSC experiments also showed that Ca^{2+} ions increased the denaturation temperatures (Fig. 2). This was as expected from previous work, which showed that the addition of Ca^{2+} ions retarded the thermal inactivation of *Tabium* CGTase.[19] Thus, the DSC experiments demonstrate that mutant 9 has a significantly higher denaturation temperature than wild-type

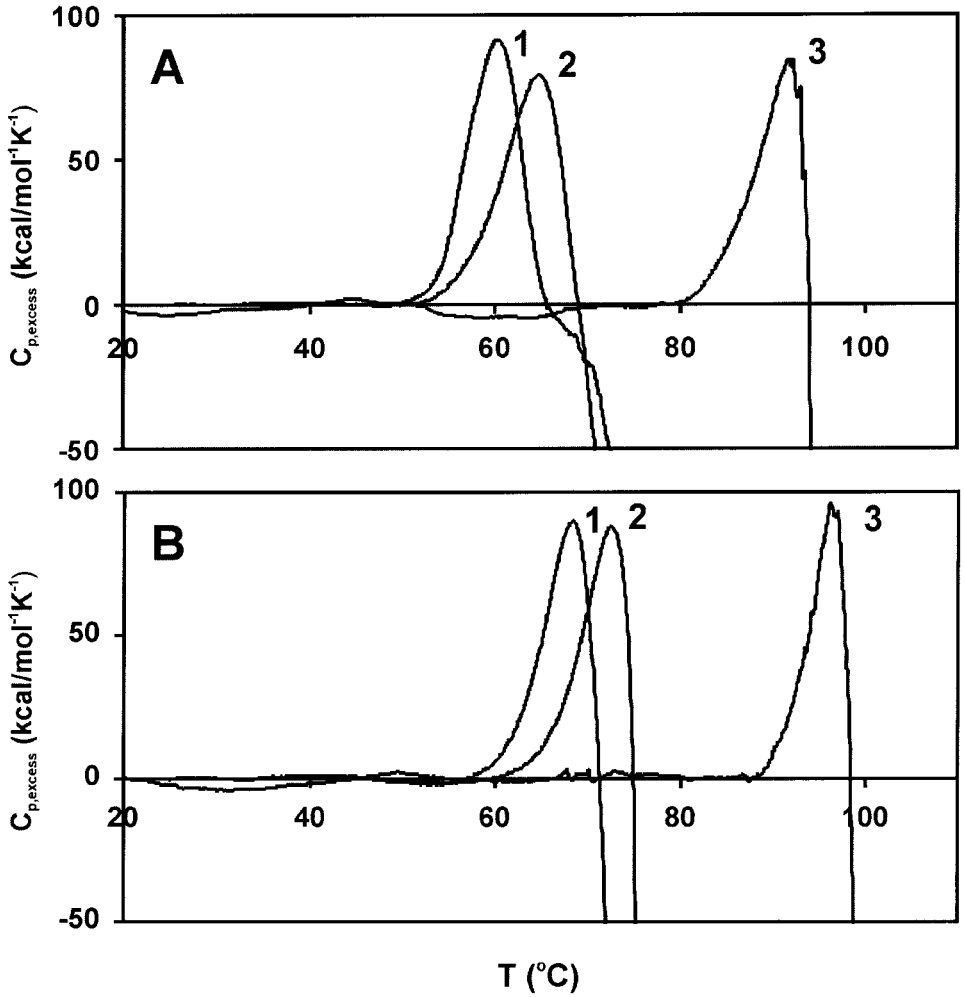

Fig. 2. DSC curves for the thermal denaturation of wild-type BC251 CGTase (1), BC251 CGTase mutant 9 (2), and *Tabium* CGTase (3), in the absence (**A**) and presence (**B**) of 10 m*M* added Ca^{2+} ions.

BC251 CGTase, although it is still much lower than that of *Tabium* CGTase.

CONCLUSIONS

Based on a comparison of the 3D structures of CGTases, we were able to increase significantly the activity half-live of BC251 CGTase via rational mutagenesis. The structure of the mutant with the largest increase in activity half-life (with N188D and K192R mutations in the B-domain) showed the presence of a salt-bridge interaction between Asp188 and Arg192, as expected from the situation in *Tabium* CGTase.

ACKNOWLEDGMENTS

Our thanks to Gea Schuurman-Wolters for assistance with the DSC measurements.

REFERENCES

1. Henrissat B, Davies G. Structural and sequence-based classification of glycoside hydrolases. Curr Opin Struct Biol 1997;7:637–644.
2. Svensson B. Protein engineering in the alpha-amylase family: Catalytic mechanism, substrate specificity, and stability. Plant Mol Biol 1994;25:141–157.
3. Takata H, Kuriki T, Okada S, Takesada Y, Iizuka M, Minamiura N, Imanaka T. Action of neopullulanase: Neopullulanase catalyzes both hydrolysis and transglycosylation at alpha-(1–4)-and alpha-(1–6)-glucosidic linkages. J Biol Chem 1992;267:18447–18452.
4. McCarter JD, Withers SG. Mechanisms of enzymatic glycoside hydrolysis. Curr Opin Struct Biol 1994;4:885–892.
5. Uitdehaag JCM, Mosi R, Kalk KH, van der Veen BA, Dijkhuizen L, Withers SG, Dijkstra BW. X-ray structures along the reaction pathway of cyclodextrin glycosyltransferase elucidate catalysis in the alpha-amylase family. Nat Struct Biol 1999;6:432–436.
6. Kuriki T, Imanaka T. The concept of the α-amylase family: Structural similarity and common catalytic mechanism. J Biosci Bioeng 1999;87:557–565.
7. Carbohydrate-active enzymes server. Available online at http://afmb.cnrs-mrs.fr/CAZY; 1999.
8. Mosi R, He S, Uitdehaag JCM, Dijkstra BW, Withers SG. Trapping and characterization of the reaction intermediate in cyclodextrin glycosyltransferase by use of activated substrates and a mutant enzyme. Biochemistry 1997;36:9927–9934.
9. Penninga D, Strokopytov B, Rozeboom HJ, Lawson CL, Dijkstra BW, Bergsma J, Dijkhuizen L. Site-directed mutations in tyrosine 195 of cyclodextrin glycosyltransferase from *Bacillus circulans* strain 251 affect activity and product specificity. Biochemistry 1995;34:3368–3376.

10. Klein C, Schulz GE. Structure of cyclodextrin glycosyltransferase refined at 2.0 Å resolution. J Mol Biol 1991;217:737–750.
11. Lawson CL, van Montfort R, Strokopytov B, Rozeboom HJ, Kalk KH, de Vries GE, Penninga D, Dijkhuizen L, Dijkstra BW. Nucleotide sequence and X-ray structure of cyclodextrin glycosyltransferase from *Bacillus circulans* strain 251 in a maltose-dependent crystal form. J Mol Biol 1994;236:590–600.
12. Knegtel RM, Wind RD, Rozeboom HJ, Kalk KH, Buitelaar RM, Dijkhuizen L, Dijkstra BW. Crystal structure at 2.3 Å resolution and revised nucleotide sequence of the thermostable cyclodextrin glycosyltransferase from *Thermoanaerobacterium thermosulfurigenes* EM1. J Mol Biol 1996;256:611–622.
13. Kubota M, Matsuura Y, Sakai S, Katsube Y. Molecular structure of *B. stearothermophilus* cyclodextrin glucanotransferase and analysis of substrate binding site. Denpun Kagaku 1991;38:141–146.
14. Harata K, Haga K, Nakamura A, Aoyagi M, Yamane K. X-ray structure of cyclodextrin glucanotransferase from alkalophilic *Bacillus* sp. 1011: Comparision of two independent molecules at 1.8 Å resolution. Acta Crystallogrs 1996;52:1136–1145.
15. Strokopytov B, Knegtel RM, Penninga D, Rozeboom HJ, Kalk KH, Dijkhuizen L, Dijkstra BW. Structure of cyclodextrin glycosyltransferase complexed with a maltononaose inhibitor at 2.6 angstrom resolution: Implications for product specificity. Biochemistry 1996; 35:4241–4249.
16. Penninga D, van der Veen BA, Knegtel RM, van Hijum SAFT, Rozeboom HJ, Kalk KH, Dijkstra BW, Dijkhuizen L. The raw starch binding domain of cyclodextrin glycosyltransferase from *Bacillus circulans* strain 251. J Biol Chem 1996;271:32777–32784.
17. Ohdan K, Kuriki T, Takata H, Kaneko H, Okada S. Introduction of raw starch-binding domains into *Bacillus subtilis* alpha-amylase by fusion with the starch-binding domain of *Bacillus* cyclomaltodextrin glucanotransferase. Appl Environ Microbiol 2000;66:3058–3064.
18. Uitdehaag JCM, Dijkstra BW. A strategy for engineering thermostability: the case of cyclodextrin glycosyltransferase. In: Ballesteros A, editor. Stability and stabilization of biocatalysts. New York: Elsevier; 1998. p 317–323.
19. Wind RD, Liebl W, Buitelaar RM, Penninga D, Spreinat A, Dijkhuizen L, Bahl H. Cyclodextrin formation by the thermostable alpha-amylase of *Thermoanaerobacterium thermosulfurigenes* EM1 and reclassification of the enzyme as a cyclodextrin glycosyltransferase. Appl Environ Microbiol 1995;61:1257–1265.
20. Fujiwara S, Kakihara H, Sakaguchi K, Imanaka T. Analysis of mutations in cyclodextrin glucanotransferase from *Bacillus stearothermophilus* which affect cyclization characteristics and thermostability. J Bacteriol 1992;174:7478–7481.
21. Pedersen S, Dijkhuizen L, Dijkstra BW, Jensen BF, Jørgensen ST. A better enzyme for cyclodextrins. Chemtech 1995;12:19–25.
22. Rashid N, Cornista J, Ezaki S, Fukui T, Atomi H, Imanaka T. Characterization of an archaeal cyclodextrin glucanotransferase with a novel C-terminal domain. J Bacteriol 2002;184:777–784.
23. Yamamoto K, Shiraki K, Fujiwara S, Takagi M, Fukui K, Imanaka T. *In vitro* heat effect on functional and conformational changes of cyclodextrin glucanotransferase from hyperthermophilic archaea. Biochem Biophys Res Commun 1999;265:57–61.
24. Tachibana Y, Kuramura A, Shirasaka N, Suzuki Y, Yamamoto T, Fujiwara S, Takagi M, Imanaka T. Purification and characterization of an extremely thermostable cyclomaltodextrin glucanotransferase from a newly isolated hyperthermophilic archaeon, a *Thermococcus* sp. Appl Environ Microbiol 1999;65:1991–1997.
25. Otwinowski Z, Minor W. Processing of X-ray diffraction data collected in oscillation mode. Methods Enzymol 1997;276:307–326.
26. Brünger AT, Adams PD, Clore GM, DeLano WL, Gros P, Grosse-Kunstleve RW, Jiamg J-S, Kuszewski J, Nilges M, Pannu NS, Read RJ, Rice LM, Simonson T, Warren GL. Crystallography & NMR system: A new software suite for macromolecular structure determination. Acta Crystallogr D 1998;54:905–921.
27. Jones TA, Zou JY, Cowan SW, Kjeldgaard M. Improved methods for building protein models in electron density maps and the location of errors in these models. Acta Crystallogr, 1991;47:110–119.
28. Meissner PS, Sisk WP, Berman ML. Bacteriophage lambda cloning system for the construction of directional cDNA libraries. Proc Natl Acad Sci U S A 1987;84:4171–4175.
29. Smith H, de Jong A, Bron S, Venema G. Characterization of signal-sequence-coding regions selected from the *Bacillus subtilis* chromosome. Gene 1988;70:351–361.
30. Sambrook J, Frisch EJ, Maniatis T. Molecular cloning: A laboratory manual. New York: Cold Spring Harbor Laboratory Press; 1989.
31. Bron S. Modern microbiological methods for *Bacillus*. In: Harwood CR, Cutting SM, editors. Plasmids. New York/Chichester: Wiley; 1990. p 146–147.
32. Leemhuis H, Dijkstra BW, Dijkhuizen L. Mutations converting cyclodextrin glycosyltransferase from a transglycosylase into a starch hydrolase. FEBS Lett 2002;514:189–192.
33. Vikmon M. Rapid and simple spectrophotometric method for determination of microamounts of cyclodextrins. In: Szejlti J, editor. First international symposium on cyclodextrins. Dordrecht, The Netherlands: Reidel Co; 1982. 64 p.
34. Nakamura A, Haga K, Yamane K. The transglycosylation reaction of cyclodextrin glucanotransferase is operated by a ping-pong mechanism. FEBS Lett 1994;337:66–70.
35. van der Veen BA, Leemhuis H, Kralj S, Uitdehaag JCM, Dijkstra BW, Dijkhuizen L. Hydrophobic amino acid residues in the acceptor binding site are main determinants for reaction mechanism and specificity of cyclodextrin glycosyltransferase. J Biol Chem 2001;276:44557–44562.
36. Guex N, Peitsch MC. SWISS-MODEL and the Swiss-Pdb Viewer: An environment for comparative protein modeling. Electrophoresis 1997;18:2714–2723.
37. Berman HM, Westbrook J, Feng Z, Gilliland G, Bhat TN, Weissig H, Shindyalov IN, Bourne PE. The Protein Data Bank. Nucleic Acids Res 2000;28:235–242.
38. Leemhuis H, Rozeboom HJ, Wilbrink M, Euverink GJW, Dijkstra BW, Dijkhuizen L. Conversion of cyclodextrin glycosyltransferase into a starch hydrolase by directed evolution: The role of Ala230 in acceptor subsite +1. Biochemistry 2003;42:7518–7526.
39. Uitdehaag JCM, Kalk KH, van der Veen BA, Dijkhuizen L, Dijkstra BW. The cyclization mechanism of cyclodextrin glycosyltransferase (CGTase) as revealed by a gamma-cyclodextrin-CGTase complex at 1.8-Å resolution. J Biol Chem 1999;274:34868–34876.
40. van der Veen BA, Uitdehaag JCM, Penninga D, Van Alebeek GJ, Smith LM, Dijkstra BW, Dijkhuizen L. Rational design of cyclodextrin glycosyltransferase from *Bacillus circulans* strain 251 to increase alpha-cyclodextrin production. J Mol Biol 2000;296:1027–1038.
41. van der Veen BA, Uitdehaag JCM, Dijkstra BW, Dijkhuizen L. The role of arginine 47 in the cyclization and coupling reactions of cyclodextrin glycosyltransferase from *Bacillus circulans* strain 251: Implications for product inhibition and product specificity. Eur J Biochem 2000;267:3432–3441.
42. Savchenko A, Vieille C, Kang S, Zeikus JG. *Pyrococcus furiosus* alpha-amylase is stabilized by calcium and zinc. Biochemistry 2002;41:6193–6201.
43. Igarashi K, Hatada Y, Ikawa K, Araki H, Ozawa T, Kobayashi T, Ozaki K, Ito S. Improved thermostability of a *Bacillus* alpha-amylase by deletion of an arginine-glycine residue is caused by enhanced calcium binding. Biochem Biophys Res Commun 1998; 248:372–377.
44. Declerck N, Joyet P, Gaillardin C, Masson JM. Use of amber suppressors to investigate the thermostability of *Bacillus licheniformis* alpha-amylase: Amino acid replacements at 6 histidine residues reveal a critical position at His-133. J Biol Chem 1990;265:15481–15488.
45. Declerck N, Machius M, Chambert R, Wiegand G, Huber R, Gaillardin C. Hyperthermostable mutants of *Bacillus licheniformis* alpha-amylase: Thermodynamic studies and structural interpretation. Protein Eng 1997;10:541–549.